

Interactions between Zn^{2+} or ZnO with TiO_2 to produce an efficient photocatalytic, superhydrophilic and aesthetic glass

**Géraldine L.-M. Léonard^a, Carlos A. Paez^a, Alfonso E. Ramírez^b,
Julien G. Mahy^a *, Benoît Heinrichs^a**

^a *Nanomaterials, Catalysis & Electrochemistry - NCE, Department of Chemical Engineering, University of Liège, B6a, Quartier Agora, Allée du six Août 13, 4000 Liège, Belgium*

^b *Grupo Catálisis, Departamento de Química, Universidad del Cauca, Popayán-Cauca, Calle 5 No. 4-70, Colombia*

***Corresponding author:** Julien G. Mahy, , Department of Chemical Engineering – Nanomaterials, Catalysis & Electrochemistry, University of Liège, B6a, Quartier Agora, Allée du six Août 13, 4000 Liège, Belgium. E-mail address: julien.mahy@ulg.ac.be . Tel: +32 4 366 35 63.

Abstract

Zinc was coupled with titanium dioxide using different methods. SiO_2 and $Zn-SiO_2$ doped TiO_2 films, on the one hand, and Zn doped TiO_2 on the other hand, have been produced using controlled sol-gel processes by alcoholic, cogelation and aqueous ways. From these syntheses, films were deposited on soda lime glass. These samples were compared to ZnO samples but also to bilayer samples constituting one layer of TiO_2 and one layer of ZnO . The physico-chemical properties of the films were characterized by grazing-incidence X-ray diffraction, profilometry and UV-Vis absorption analyses. The photocatalytic activity has been evaluated from the degradation of methylene blue under UV-A light, from the degradation of *p*-nitrophenol under visible light and from the degradation of H_2O_2 under halogen light (UV-A + visible light). Superhydrophilicity was evaluated from contact angle measurement after UV

exposition and also from hysteresis effects. Finally, a haze measurement was performed to evaluate the impact of the coating on the aesthetic property of the coated glass.

Aqueous films have better photocatalytic activity and superhydrophilicity than samples from alcoholic synthesis. The crystallization of the sample appears to be one key factor: alcoholic films required calcination to ensure the crystallization of TiO_2 , but the alkali migration from the glass support prevents this crystallisation, while aqueous synthesis promotes crystallized particles at low temperatures without alkali interference.

It appears that the relative activity from one sample to another depends on the nature of the illumination and on the nature of the molecule to be degraded. Nevertheless, the sample with ZnO layer deposited on first TiO_2 layer (ZnO 500 Alc/ TiO_2 100 AQ) composite is found to be the best sample, maintaining a high hydrophilicity similar to TiO_2 and a good activity.

Keywords

TiO_2 , Zn^{2+} , ZnO , superhydrophilicity, photocatalysis, hydrogen peroxide decomposition

1. Introduction

Nowadays, the need to reduce pollution is important. Different methods are used for this purpose and in this work the advanced catalytic oxidation process (AOP) with doped catalysts was examined to reduce the pollutant amount [1-5]. The material used in one form of the process is a photocatalyst in the form of a powder or a film. When a photocatalyst is exposed under adequate light [6], electrons from the valence band are promoted to the conduction band. Positive holes are thus produced in the valence band. Both, electrons and holes, at the surface of the catalyst, can produce radical species such as $\text{O}_2^{-\bullet}$ and OH^{\bullet} from reactions with adsorbed O_2 and H_2O . Those radicals can then promote pollutant degradation.

In this study, two photocatalysts were studied and compared: ZnO and TiO₂. These two photocatalysts, with similar band gap (TiO₂ anatase band gap = 3.2 eV and ZnO band gap = 3.4 eV), are cheap, non-toxic, environmentally friendly and possess good chemical and thermal stability [7-10].

From an electronic point of view, ZnO and TiO₂ are the best semiconductor candidates. Indeed, the valence band and the conduction band of ZnO are constituted of *d* orbitals and *sp* hybrid orbitals respectively. TiO₂ is constituted of *p* orbitals hybridized with *d* orbitals in the valence band and of *d* orbitals only in the conduction band. These two configurations are in favour of an efficient electron-hole pair promotion. The configuration of ZnO induces a dissimilar parity of the electrons in the valence and conduction bands that decreases the recombination of electrons and holes; TiO₂ has electrons in valence and conduction bands with different parities also inducing a decrease in the recombination of electrons and holes [11]. However, despite these configurations, the reduced recombination is not negligible. Previous comparisons of TiO₂ and ZnO have shown a variety of reported results. In some studies, ZnO has a lower rate of recombination compared to TiO₂ [11, 12].

A brief review of the literature on photocatalytic performances reporting TiO₂ and ZnO efficiencies highlights a range of different results. ZnO is more active than TiO₂, for example, in the degradation of glucose under UV [13] and for the degradation of acid brown 14 (C₂₆H₁₆N₄Na₂O₈S₂) due to a better absorption of light quanta [14]. In some other cases, TiO₂ is the best. For example, TiO₂ is better than ZnO for the degradation of 4-chlorophenol under Hg lamp [15], for the degradation of methylorange [16] and for the decomposition of NO_x due to a better photoconductivity [17, 18]. It is therefore difficult to predict which material is the best catalyst for the degradation of a specific molecule under a specific illumination.

In the present study, the catalyst was shaped in the form of a film. Despite the lower amount of matter, films have the advantage of avoiding the separation step which is needed when powders

are used in batch reactors. When photocatalytic films are produced, another important property, can be very useful for some applications, and it is the photoinduced superhydrophilicity.

Superhydrophilicity is induced mainly by photogenerated holes. These holes can weaken bonds between oxygen and the metal (Ti or Zn), inducing the promotion of oxygen vacancies which promote adsorption of water, and so the formation of -OH superficial groups. These hydroxyl groups have a high affinity with water, promoting the formation of a water film instead of a drop [19-21]. Superhydrophilicity is characterized by a low contact angle (<10°) while hydrophilicity is characterized by a contact angle between 10° and 90°. The superhydrophilic propertiy of the film does not depend on film composition only but also on surface properties such as roughness [22].

Superhydrophilicity of TiO_2 has been widely investigated. Different results have been obtained when comparing ZnO and TiO_2 . In the literature, TiO_2 can be more efficient than ZnO [18] but comparisons between the two have not been very rigourously in details under different conditions. Some results have indicated that in the dark, ZnO can reach very high water contact angles [23-25] compared to TiO_2 .

Additionally, in the case of coatings on glass, one important point is the final aesthetic aspect and the preservation of transparency, which has been evaluated by haze measurement.

With the aim of developing a highly photoactive and superhydrophilic material, this study sets out to compare samples of TiO_2 , from alcoholic or aqueous synthesis, with ZnO . Knowing that, according to literature, TiO_2 can be more hydrophilic and ZnO more photoactive in some cases, and less active in others cases, different samples combining different species of TiO_2 and ZnO are investigated. Such combinations can be achieved using different methods.

First, Zn^{2+} can be introduced in a TiO_2 matrix. From the literature, the introduction of metal ions such as Zn^{2+} into TiO_2 can induce a weakening of oxygen bonds resulting in the departure

of the oxygen and so, therefore, in oxygen vacancies. These oxygen vacancies play different roles. First, they can induce the adsorption and the dissociation of water resulting in a high OH density at the surface that can promote photoactivity and superhydrophilicity [26]. The departure of oxygen can also promote the trapping of photogenerated holes and increase the lifetime of photogenerated electrons [27].

More generally, Zn^{2+} can act directly by decreasing the recombination of electrons and holes: Zn^{2+} can trap a photogenerated electron ($Zn^{2+} + e^- \rightarrow Zn^+$). Zn^+ can then react with oxygen by electron transfer ($Zn^+ \rightarrow Zn^{2+} + e^-$) or Zn^+ can trap a photogenerated hole ($Zn^+ + h^+ \rightarrow Zn^{2+}$). Another mechanism is the trapping of a hole by Zn^{2+} ($Zn^{2+} + h^+ \rightarrow Zn^{3+}$). Zn^{3+} can then react with OH^- to produce radicals or directly degrade organic pollutant by the Fenton process [26, 28]. Moreover, the introduction of Zn^{2+} ensures not only the presence of Zn^{2+} but can also result in the formation of ZnO which has an intrinsic photoactivity for the degradation of pollutants in addition to TiO_2 [26, 29]. Zn^{2+} can also act on TiO_2 structure: for example, in some cases, it has led to a particle size decrease inducing a better activity (quantum effect and surface area) [27-29]. Finally, Zn^{2+} can also induce a red shift of TiO_2 absorption due to the creation of impurity levels in the band gap of TiO_2 [28].

To do this doping, two syntheses of TiO_2 were tested with different synthesis protocols and dopant incorporation. A perfectly controlled sol-gel method was used to produce TiO_2 -based catalysts containing zinc. Previous works have reported that a high dispersion of ions into a SiO_2 powder matrix can be achieved through the use of a complexing agent, such as ethylenediamine [30]. That method, the cogelation way, has already been used to dope TiO_2 with silver [31]. By using zinc acetate as the zinc source, ions can be complexed by the amine group of an alkoxy silane-functionalized ligand such as N-[3-(trimethoxysilyl)propyl]ethylenediamine (EDAS). Thanks to its alkoxy groups, the “ Zn^{2+} - EDAS” complex can therefore react with a titanium alkoxide precursor during the hydrolysis

and condensation reactions. This allows anchoring of Zn^{2+} ions onto the TiO_2 surface through the formation of Ti-O-Si chemical bonds (Figure 1). After calcination, which is required to obtain crystalline TiO_2 , the material contains exclusively TiO_2 into which SiO_2 and zinc are dispersed.

Another synthesis was aqueous synthesis. In this case, titanium alkoxide has been dispersed in acidic water (HNO_3) to induce TiO_2 precipitation. The dopant was incorporated in the form of nitrates. After a soft thermal treatment inducing peptization, a stable sol was obtained, which was composed of very small anatase crystallites with highly dispersed Zn^{2+} ions [26, 32].

In addition to the incorporation of Zn^{2+} into the TiO_2 matrix, a second combining can be achieved. TiO_2 and ZnO can be directly coupled together. The combination of two semiconductors, as already explained in the literature, decreases the recombination of the electron-hole pairs. Indeed electrons can migrate between the conduction bands and holes can migrate between the valence bands of TiO_2 and ZnO [7]. Different configurations have been observed depending on the relative position of the bands. For example, in some cases, electrons go from the conduction band of TiO_2 (e.g. -4.21 eV) to the conduction band of ZnO (e.g. -4.19 eV) and inversely the holes can go from the valence band of ZnO (e.g. -7.39 eV) to the valence band of TiO_2 (e.g. -7.41 eV) [13, 15, 33]. The delocalization of photogenerated charges decreases their recombination. On the opposite, in other cases, the mechanism is the inverse: electrons go from the ZnO to the TiO_2 conduction band and holes go from the TiO_2 to ZnO valence band [34-36]. The configuration depends on the position of the bands, which depends on each system. Indeed, the morphology of the catalyst through the synthesis conditions (precursor, solvent, ...) and thermal treatments, as well as the presence of defects, can all influence the energetic configuration [36].

Another effect resulting from the coupling of ZnO and TiO_2 is a shift of light absorption to visible wavelengths [7, 13, 33, 35]. Additionally, the combination of ZnO with TiO_2 induces

an enhancement of the activity through the creation of oxygen vacancies [18, 35, 37]. Finally the combination induces modification of textural properties in favour of a better superhydrophilicity and a better H₂O adsorption [22].

In this study, one method used to create a hybrid TiO₂/ZnO material was the manufacture of a two layer material. It is hypothesized that two successive layers could be better than one single layer mixing ZnO and TiO₂. Indeed, for example, during calcination of a layer containing both TiO₂ and ZnO, low crystallizations of TiO₂ or ZnO have been observed due to the presence of both metal oxides [16-18]. In the case of bilayer samples, TiO₂ can be deposited before or after the ZnO layer, allowing a first calcination of a pure TiO₂ or ZnO layer respectively.

To summarize, the main objective of this work was to develop a material TiO₂ and ZnO-based with a high photocatalytic activity and a high superhydrophilicity with the smallest change in aesthetical appearance.

2. Experimental

2.1. Preparation of sols

2.1.1. TiO₂ with Alcoholic (and cogelation) synthesis

All alcoholic syntheses (**Alc**) have been performed at room temperature in a constant nitrogen flow in order to avoid precipitation of the titanium precursor through reactions with ambient humidity. The TiO₂ sol was prepared using titanium tetraisopropoxide (TTIP > 97 %, Aldrich), anhydrous 2-methoxyethanol (Methoxyethanol ACS 99.3+ %, Alfa Aesar) and ultrapure water as starting materials (Figure 2).

In the case of pure alcoholic TiO₂, 7.79 mL of TTIP was added to one half of the solvent, 48 mL, and vigorously stirred for 30 min in a first vessel. In a second vessel, a small amount of

deionised water, 1.16 mL was dissolved into the second half of solvent, 48 mL. After 30 min of stirring, the water-containing solution was added to the first vessel in order to induce the hydrolysis and condensation reactions, and the final mixture was stirred vigorously for 1 h. Stable colloidal suspensions suitable for film deposition were obtained (TiO₂ Alc) and placed inside a glovebox (MB 200B, mBrAun, argon atmosphere, T = 17°C, [H₂O] < 0.1 ppm, [O₂] < 0.1 ppm).

In the case of TiO₂-SiO₂-Zn sols, 0.724 mL of N-[3-(trimethoxysilyl)propyl]ethylenediamine (EDAS for synthesis, Merck) was added to a first vessel containing one half of the solvent (46 mL) and then 0.37 g of zinc acetate (Zn(C₂H₃O₂)₂*2H₂O, zinc acetate dihydrate for synthesis, EMSURE®, Merck) was added to the EDAS solution. After complete dissolution/complexation of zinc (homogeneous solution), TTIP was added and stirring was maintained for 30 min before adding the water-containing solution. The total amount of Zn²⁺ was 5 wt%.

For comparison and control purposes, SiO₂-TiO₂ sols were synthesized. In this case, N-[3-(trimethoxysilyl)propyl]ethylenediamine (EDAS for synthesis, Merck) was dissolved into a first vessel containing one half of the solvent in order to obtain a sample with the same amount of SiO₂ as in the sample containing both SiO₂ and Zn. When the solution was perfectly homogeneous, TTIP was then added to the mixture and stirring was continued for 30 min before adding the solution-containing water.

2.1.2. TiO₂ with aqueous synthesis

For aqueous synthesis (AQ) (Figure 3), prepared at ambient atmosphere, 28.5 g of TTIP (TTIP > 97 %, Aldrich) stabilized with acetic acid (Acetic acid (glacial) 100 % EMPROVE®, Merck) was incorporated in ultrapure water.

The obtained white precipitate was washed three times with ultrapure water. Finally, 19.5 g of 1 M HNO₃ (solution prepared from: nitric acid 65 % Suprapur, Merck) and 13.7 g of 0.5 M Zn(NO₃)₂ solution (solution prepared from: Zn(NO₃)₂*6H₂O, zinc nitrate hexahydrate reagent grade 98 %, Sigma-Aldrich) were added (HNO₃ only for pure TiO₂). The resulting solution was vigorously stirred at 45 °C for 16 h to induce TiO₂ peptization. The final sol was kept in ambient atmosphere.

2.1.3. ZnO synthesis

The zinc precursor, zinc acetate (Zn(C₂H₃O₂)₂*2H₂O, zinc acetate dihydrate for synthesis, EMSURE®, Merck), was added 250 mL of ethanol. The solution was stirred and 4.49 mL of monoethanolamine (MEA, ethanolamine, purified by distillation, > 99.5 %) was added to reach a mole ratio of Zn²⁺:MEA=1 in order to stabilize the solution. The solution was homogenized and heated to 70 °C for 1 h before cooling to room temperature. The obtained sol was transparent (Figure 4).

2.2. Preparation of films

2.2.1. Film deposition

The films were produced by dip-coating. Coating parameters were adjusted to obtain similar thicknesses for both alcoholic and aqueous syntheses. Soda lime glass (pieces of 75 x 25 x 4 mm) was used as a support, to simulate industrial application.

For pure TiO₂ from alcoholic synthesis (Alc), another thickness of glass piece (75 x 25 x 2 mm) was also used to test the influence of the substrate.

In the case of TiO₂ aqueous synthesis (AQ), the glass surface was pre-treated to ensure adherence of the sol. The glass pieces were immersed in an H₂SO₄/H₂O₂ acid solution (molar ratio: 3:1) and abundantly washed with water. Surfaces obtained after such a pre-treatment are

completely fat-free and more hydrophilic. In the case of TiO_2 alcoholic, and ZnO synthesis, calcination is required after deposition to obtain crystalline phases (anatase or zincite). The use of glass containing alkali can be harmful due to sodium and calcium diffusion during the thermal treatment, preventing a good crystallization. A solution for this problem is to deposit a SiO_2 barrier layer that prevents sodium and calcium from migrating to the crystallizing active layer. The SiO_2 solution was obtained by mixing 45 mL of water with 120 mL of ethanol. After homogenization, 1.35 mL of chlorhydric acid was added. After 15 min, 100 mL of silicon precursor, tetraorthosilicate (TEOS, Sigma-Aldrich®, 98%) was added. After 30 minutes of stirring, the solution was ready. Such a solution remains stable only for approximately one month.

The glass pieces were dipped at 60 mm/min and withdrawn at: 60 mm/min for SiO_2 synthesis, 60 mm/min for TiO_2 alcoholic (and cogelation) synthesis, 10 mm/min for TiO_2 aqueous synthesis and 60 mm/min for ZnO synthesis, respectively. The films obtained were left at ambient temperature for 200 s to dry. Only monolayer films were produced to ensure transparency.

2.2.2. Thermal treatment

Table 1 summarizes the different sorts of produced film. Samples were named ABC/A'B'C'. The different layers were classified by their chemistry (A for the last layer and A' for the first deposited layer), the thermal treatment applied (B for the last layer and B' for the first deposited layer) and the synthesis (C for the last layer and C' for the first deposited layer).

After drying, the films obtained were heated in air at different temperatures. SiO_2 sublayers were heated at 100°C to evaporate the solvent and to ensure the adherence of the SiO_2 layer during the deposition of the second layer. Films from TiO_2 alcoholic synthesis (Alc), with or without SiO_2 sublayer, were calcined at 500°C (TiO_2 500 Alc, TiO_2 500/Alc SiO_2 100 Alc,

TiO₂-SiO₂ 500 Alc/ SiO₂ 100 Alc and TiO₂-SiO₂-Zn 500 Alc/ SiO₂ 100 Alc films) for 1 h with the aim of removing organic species and trying to obtain anatase phase. Films from aqueous (AQ) synthesis were already crystallized in anatase after deposition but were heated at 100°C (TiO₂ 100 AQ and TiO₂-Zn 100 AQ) or calcined at 500°C (TiO₂ 500 AQ and TiO₂-Zn 500 AQ) in order to study the adherence of the film and to remove water.

Composite films composed of aqueous TiO₂ and ZnO were also tested (Figure 5). Three composites were produced: ZnO 60 mm/min dried at 100°C with then TiO₂ 10 mm/min as a second layer and final calcination at 500°C (TiO₂ 500 AQ/ZnO 100 Alc); ZnO 60 mm/min calcined at 500°C with then TiO₂ 10 mm/min as a second layer and a final calcination at 500°C (TiO₂ 500 AQ/ZnO 500 Alc); TiO₂ 10 mm/min dried at 100°C with then ZnO 10 mm/min as a second layer and a final calcination at 500°C (ZnO 500 Alc/TiO₂ 100 AQ).

2.3. Characterization of films

The crystallinity has been characterized by grazing incidence X-Ray diffraction (GIXRD) in a Bruker D8 diffractometer using Cu radiation and operating at 40 kV and 40 mA. The incidence beam angle was 0.25°. The Scherrer formula was used to determine the size of TiO₂ crystallites, d, from the peak broadening:

$$d = 0.9 \frac{\lambda}{B \cos(\theta)} \quad (\text{Eq. 1})$$

where d is the crystallite size [nm]; B is the full-width at half maximum after correction from the instrumental broadening [rad]; λ is the wavelength [nm]; and θ is the Bragg angle [rad].

The thickness and roughness of films were evaluated by profilometry with a Veeco Dektak 8 Stylus profilometer. To obtain reliable and representative results, for each type of film, three samples were analysed; three spots were examined in each sample and ten runs were performed on each spot.

The optical properties of the films were studied through **UV-Vis absorption spectroscopy** (Genesys 10S, Thermo Scientific) between 250 nm to 800 nm.

It is desirable that any coating should not change the glass aesthetical aspect. The measurement of the haze reveals the optical effect of the coating on the glass. Haze measurements were performed with a hazemeter (Haze-gard plus from BYK) on three samples. Measuring haze allows the characterization of the behaviour of the light when wide angle scattering occurred. Light is so diffused in all directions causing a loss of contrast. Haze is defined as the percentage of light which deviates more than 2.5 degrees on average compared to the incident beam. The intensity of the incidence beam must be corrected by subtraction of the reflection and the absorption of the material. Haze is thus defined by this ratio:

$$\text{Haze} = \frac{\text{Tr}_{\text{diff}}}{\text{Tr}_t} \cdot 100 \% \quad (\text{Eq. 2})$$

where Tr_{diff} is the diffuse transmittance ($> 2.5^\circ$) and Tr_t is the total transmittance (Incidence beam after the reflection and absorption are subtracted).

2.4. Photocatalytic activity

2.4.1. Degradation of methylene blue and *p*-nitrophenol

The photocatalytic activity of the films has been evaluated by monitoring the degradation of methylene blue (MB) under UV-A light (Osram Sylvania, Blacklight-Bleu Lamp, F18W/BLB-T8), and of *p*-nitrophenol (PNP) under visible light (SECYS halogen reflector GUS 3, 50 W 12 V with UV filter removing wavelengths below 390 nm) over 24 h. The spectra of the lamps was measured with a Hamamatsu TG mini-spectrophotometer and the intensity with a radiometer from Equipement Scientifique equipped with PMA 2100- UVA-B PMA 2107 detectors. UV-A light can be considered as monochromatic with a wavelength $\lambda = 365$ nm and

an intensity of 1.2 mW/cm². Visible light (halogen light + UV filter) has a range from 400 nm to 800 nm and has an intensity of 77 mW/cm².

Each film (Substrate 7.5 x 2.5 cm – Coated 6 x 2.5 cm) was placed in a petri dish (batch reactor) with 40 mL of MB 2 10⁻⁵ M solution for the UV-A test and PNP 10⁻⁴ M solution for visible light test. The evolution of MB or PNP concentration was evaluated from absorbance measurements with a Genesys 10S UV-Vis spectrophotometer (Thermo Scientific) at $\lambda = 665$ nm for MB (maximum of absorbance) and at $\lambda = 317$ nm for PNP (maximum of absorbance of the PNP acid form). Preliminary adsorption tests performed in the dark (dark tests) showed that PNP is not significantly adsorbed on the surface of the different catalysts, contrary to MB which presents a weak adsorption. A blank test consisting of irradiating the pollutant solution for 24 h in a petri dish without any catalyst showed a very weak degradation of MB under UV-A illumination (5 %), while PNP under visible light remained intact.

The batch reactors with catalyst and pollutant were stirred on orbital shakers and illuminated for 24 h. Aliquots of MB and PNP solutions were sampled every hour. The photocatalytic degradation is equal to the total degradation from which the degradation without catalyst (blank test) and the adsorption value on catalyst (dark test) are subtracted. Curves of MB and PNP concentrations as a function of time then have allowed the kinetic constant to be calculated, assuming a first order kinetics.

Each measurement of the photocatalytic activity was replicated three times in order to assess the reproducibility of the data.

2.4.2. Degradation of hydrogen peroxide to oxygen

The photocatalytic activity of the films was also determined from the degradation of H₂O₂ in aqueous solution [38]. The volume of oxygen produced per time unit at atmospheric pressure was measured during illumination of a sample placed in H₂O₂ solution. The photoreaction was

carried out using a batch reactor with halogen lamp (300 W, 230 V) powered at 110 V. The emission spectrum of the halogen lamp (300 W, 230 V) was measured with a MiniSpectrometer (Hamamatsu Photonics). The film was suspended inside the reactor with 80 mL of H₂O₂ solution (H₂O₂, 32 wt%, Merck) and the reactor was closed with a septum port and thermostated at 20°C. The initial pressure in the reactor was atmospheric pressure. The lamp was turned on. With a graduated volume, the volume of oxygen produced was recorded each minute during the first 10 min and every 5 min during the next 20 min.

The degradation was estimated from the volume of oxygen produced. Following the perfect gas law, the amount of oxygen in mole can be evaluated [38]. This amount of oxygen is directly linked to the activity of the photocatalyst.

H₂O₂ reacts due to photoactivity but also due to the direct photolysis of H₂O₂ under light. So to evaluate the amount of O₂ produced by the photocatalytic degradation, a blank test was performed to remove the contribution of O₂ produced by photolysis.

2.5. Superhydrophilicity

Superhydrophilicity was evaluated by measuring the contact angle between a droplet of water (15 μ L) and a film using a goniometer (DGB 60 Fust from GBX). Superhydrophilic materials are characterized by a contact angle lower than 10° which corresponds to a high spreading of the water droplet.

In preparation, all films were illuminated for 16 h with UV light (Philips original home solaria equipped with 15 W sunlamp Philips, 13 mW/cm²) to induce superhydrophilicity of TiO₂ or ZnO. The contact angle was then measured (A_{UV}).

Only for adherent film, after those measurements, samples were then kept for a long period (several months) in the dark. New contact angles were then measured after a short illumination under UV ($A_{UV'}$).

After these measurements on adherent films, an evaluation of the contact angle hysteresis has been measured. This measurement allows for a characterization of the chemical or/and physical surface heterogeneities. A droplet of water (15 μL) was deposited on the coating. Water was then incrementally injected into the droplet, so the contact angle increased slowly until the contact line moved. The angle at that moment is the advancing (maximal) contact angle. The inverse experiment was then performed by decreasing the amount of water in the droplet. The angle decreases until the contact line moves; the receding (minimal) contact angle. Hysteresis is the difference between the advancing and the receding contact angle (Hyst). When hysteresis is low, the film does not prevent the drop from moving freely and it means that the chemical or physical heterogeneity of the surface is low. Inversely, if the hysteresis is high, the drop is not able to move so easily due to chemical or physical heterogeneity.

3. Results

3.1. Characteristics of films

3.1.1. Physical aspect

All films are crack free and their adherence, tested by scotch test, is validated. When films are scrubbed with Tork paper, those from TiO_2 alcoholic synthesis and ZnO synthesis are still adherent but films from TiO_2 aqueous synthesis (TiO_2 100 AQ and TiO_2 -Zn 100 AQ) lose their high adherence. Calcination at 500 °C enables TiO_2 aqueous synthesis (TiO_2 500 AQ and TiO_2 -Zn 500 AQ) to obtain their high adherence.

3.1.2. X-Ray diffraction

The GIXRD patterns are shown for alcoholic synthesis, aqueous synthesis and ZnO -based syntheses in Figures 6a, 7 and 8 respectively. For pure alcoholic synthesis, the use of a silica

barrier layer does not allow crystallization of TiO_2 in anatase: indeed, no peak around 25° for TiO_2 500 Alc and TiO_2 500 Alc/ SiO_2 100 Alc can be detected on Figure 6a.

The insertion of SiO_2 (EDAS) and SiO_2 -Zn do not change the amorphous phase: no peak on Figure 6a for TiO_2 - SiO_2 500 Alc/ SiO_2 100 Alc and TiO_2 - SiO_2 -Zn 500 Alc/ SiO_2 100 Alc).

However, when the substrate is different (TiO_2 500 Alc/ SiO_2 100 Alc **2 mm**), the barrier layer prevents the alkali migration and TiO_2 crystallizes in the anatase form (peak at 25.2° on the Figure 6b).

For aqueous synthesis, all patterns in Figure 7 are similar. The peak at 25.2° from anatase is present but weaker and broader than for alcoholic synthesis on 2 mm glass (Figure 6b), indicating the presence of smaller crystallites. The crystallite size, calculated with a large error because peaks are not well defined, is around 7 nm.

Finally, ZnO is in the form of zincite phase as evidenced by the three peaks (at 31.7° , 34.3° and 36.1° for ZnO 500 Alc and ZnO 500 Alc/ SiO_2 100 Alc samples in Figure 8). A fourth peak, with a weaker intensity can be also detected at 47.4° . The crystallite size in the three directions (100), (002) and (101) is the same: 10-13 nm. When composite films are examined (Figure 8), the peaks observed are different depending on the sample. For composite film with ZnO as first layer and TiO_2 as second layer (TiO_2 500 AQ/ ZnO 100 Alc and TiO_2 500 AQ/ ZnO 500 Alc), anatase only is detected. The peaks are very weak and no crystallite size can be estimated because the margin of error is too high. GIXRD pattern of film with TiO_2 as first layer and ZnO as second layer (ZnO 500 AQ/ TiO_2 100 AQ) shows peaks of TiO_2 and ZnO . Again the precision is too low to evaluate crystallite size.

3.1.3. UV-Visible absorption

UV-Visible absorbance results are shown in Figure 9.

Untreated glass is first measured for blank test. The glass, a soda lime glass, absorbs a wide range of wavelengths in the UV. If the coating on the glass surface absorbs less than glass, it cannot be detected and the final product (glass+layer) will have the same absorption spectrum as glass. This is the case for ZnO 500 Alc. Other samples, with TiO₂, absorbs exactly in the range that is red shifted compared to ZnO alone due to TiO₂ presence.

3.1.4. Profilometry

Evaluations of the thickness and roughness of films are presented in Table 2. For bilayer films, the thickness of the first layer, the second layer and the total layer (two layers combined) are shown when measurement is possible. The reported roughness is always the total (all layers combined) roughness.

First, for TiO₂ alcoholic synthesis samples, the thickness of the TiO₂ layer is always around 50 nm with or without a SiO₂ barrier layer and with or without dopants. The roughness of films is low for all samples except for TiO₂ 500 Alc /SiO₂ 100 Alc (15 nm). For TiO₂ aqueous films, thickness is around 15 nm except for TiO₂ 500 AQ which has a greater thickness (32 nm). The roughness is very low for all films and is comparable to TiO₂ from alcoholic synthesis. ZnO 500 Alc film has a thickness of 22 nm, between the mean thickness of TiO₂ from alcoholic and aqueous synthesis, while the roughness is similar to TiO₂ syntheses. ZnO 500 Alc/TiO₂ 100 AQ composite has a thicker layer of TiO₂ than ZnO. The TiO₂ layer is not affected by the ZnO layer. Indeed, a comparison with TiO₂ 500 AQ samples shows that thicknesses are in the same range with or without ZnO. The ZnO layer is very thin, and thinner than when ZnO is deposited on glass directly. The global roughness is also increased. The characteristics of the two other TiO₂/ZnO composite films (TiO₂ 500 AQ/ZnO 100 Alc and TiO₂ 500 AQ/ZnO 500 Alc) are difficult to determine because the transition between the layers is not clearly defined. Indeed, the two layers are not perfectly superposed and it is not possible to estimate the different

thicknesses. The first layer has a thickness of around 30 nm but after deposition of the second layer, the global thickness is around 10 nm for TiO_2 500 AQ/ZnO 100 Alc and 30 nm for TiO_2 500 AQ/ZnO 500 Alc. It seems that the ZnO layer is attacked by TiO_2 . The roughness of samples is very low.

3.1.5. Aesthetic measurements

The haze of all samples with a coating is equal or nearly equal to that of the initial control glass. Therefore these measurements show that such layers do not modify the transparency of the glass. Aesthetical properties are thus kept intact.

3.2. Photocatalytic activity of films: Methylene blue and *p*-nitrophenol degradation

For all samples, the *p*-nitrophenol concentration after 24 h of reaction under visible light remain unchanged, indicating that visible light does not excite the catalyst. There is no photosensitisation to visible light of the catalyst.

The degradation of methylene blue by alcoholic TiO_2 films, aqueous TiO_2 films and ZnO-based films only is illustrated on Figure 10, 11 and 12 respectively and the conversions after 24h only due to photocatalytic activity are given in the Table 2.

From these curves, in order to compare activities of the different samples under UV light, kinetic constants have been determined assuming first order kinetics following the method that Pirard *et al.* especially developed for photocatalytic films in this reactor [39].

$$C = C_0 e^{-\frac{k S_{\text{substrate}} t}{V_0}} \quad (\text{Eq. 2})$$

where C is the pollutant concentration (kmol m^{-3}), C_0 the initial pollutant concentration (kmol m^{-3}), k is the reaction rate constant of the film ($\text{m}^3 \text{h}^{-1} \text{m}_{\text{substrate}}^{-2}$), $S_{\text{substrate}}$ is the surface of the

substrate covered by the catalytic film ($S_{\text{substrate}} = 15 \times 10^{-4} \text{ m}_{\text{substrate}}^2$) and V_0 is the initial volume of the solution ($V_0 = 25 \times 10^{-6} \text{ m}^3$).

Values of kinetic constant normalized by the surface of coated glass (k) are given in Table 2. Samples synthesized in alcohol have a very low activity. $\text{TiO}_2\text{-SiO}_2\text{-Zn 500 Alc/SiO}_2 100 \text{ Alc}$ has the highest conversion and the kinetic constant is also higher than for pure film $\text{TiO}_2 500 \text{ Alc/SiO}_2 100 \text{ Alc}$, although it is still low.

Considering the Table 2, films from aqueous syntheses are more active than those from alcoholic syntheses. Calcination in aqueous synthesis induces a decrease of the activity ($\text{TiO}_2 100 \text{ AQ} > \text{TiO}_2 500 \text{ AQ}$ and $\text{TiO}_2\text{-Zn 100 AQ} > \text{TiO}_2\text{-Zn 500 AQ}$) as illustrated in Table 2 and in Figure 11, while the introduction of Zn^{2+} does not modify significantly the kinetics ($\text{TiO}_2 100 \text{ AQ} \approx \text{TiO}_2\text{-Zn 100 AQ}$ and $\text{TiO}_2 500 \text{ AQ} \approx \text{TiO}_2\text{-Zn 500 AQ}$). The most active sample is pure ZnO 500 Alc film if the kinetic constants in the Table 2 are considered. The composites with ZnO as first layer and TiO_2 as second layer ($\text{TiO}_2 500 \text{ AQ/ZnO 100 Alc}$ and $\text{TiO}_2 500 \text{ AQ/ZnO 500 Alc}$) have activities similar to that of the sample with a TiO_2 layer only ($\text{TiO}_2 500 \text{ AQ}$) (see Figure 12). Sample with TiO_2 as first layer and ZnO as second layer ($\text{ZnO 500 Alc/TiO}_2 500 \text{ AQ}$) has an activity which slightly higher activity than that of $\text{TiO}_2 500 \text{ AQ}$ only, but also clearly lower than that of ZnO 500 Alc alone (Figure 12 and Table 2).

3.3. Photocatalytic activity of films: H_2O_2 degradation

Only samples with good adherence have been tested (No $\text{TiO}_2 \text{ AQ}$ without calcination). Moreover, from the previous photocatalytic results, only the best samples have been tested for the degradation of H_2O_2 : $\text{TiO}_2 500 \text{ AQ}$, ZnO 500 Alc , $\text{ZnO 500 Alc/TiO}_2 100 \text{ AQ}$. Firstly, the degradation of H_2O_2 only due to light is measured. Then, the degradation of H_2O_2 with light and the photocatalyst is measured. The subtraction of the light contribution is performed and so the photocatalytic contribution is evaluated. Figure 13 shows only the photocatalytic

contribution. Due to experimental errors, a significant difference between ZnO 500 Alc and TiO₂ 500 AQ cannot be detected and similar activity for both are recorded. On the other hand, the ZnO 500 Alc/TiO₂ 100 AQ composite has a higher activity.

3.4. Superhydrophilicity of films

The contact angle of samples after the first (A_{UV}) and second (A_{UV'}) UV illumination and the hysteresis (Hyst) contact angle are presented in Table 2. Except for SiO₂/TiO₂-SiO₂ 500 Alc, all samples from alcoholic syntheses (TiO₂ 500 Alc, SiO₂/TiO₂ 500 Alc and SiO₂/TiO₂-SiO₂-Zn 500 Alc) are superhydrophilic (A_{UV} < 10°). Over time, the average contact angle increases and the films are no more superhydrophilic after UV illumination (A_{UV'} > 40°). The hysteresis angles (Hyst > 30°) are large, indicating the presence of surface heterogeneities.

Films from aqueous synthesis without calcination (TiO₂ 100 AQ and TiO₂-Zn 100 AQ) have a very low angle after first illumination (A_{UV} < 10°). The contact angle is even ~0° (A_{UV}) for calcined films (TiO₂ 500 AQ and TiO₂-Zn 500 AQ). For adherent films, calcined at 500 °C, the A_{UV'} and Hyst are evaluated. Over time, this angle increases too as for alcoholic synthesis (A_{UV'} > 25°). In the case of the two syntheses of TiO₂, the angle with time still corresponds to hydrophilic samples. The hysteresis of TiO₂-Zn 500 AQ and TiO₂ 500 AQ are larger than for alcoholic synthesis.

ZnO-based films also exhibited different behaviours. All films are first hydrophilic (10 ° < A_{UV} < 20°). ZnO then loses this high hydrophilicity over the time (A_{UV'} = 28°), as do other syntheses, and has a high hysteresis (Hyst = 39°). TiO₂ 500 AQ/ZnO 100 Alc and TiO₂ 500 AQ /ZnO 500 Alc keep this hydrophilicity (A_{UV'} = 10°) and have a low hysteresis meaning that the contact line moves easily, indicating the presence of few heterogeneities. Finally, the ZnO 500 Alc/TiO₂ 100 AQ composite keeps the same hydrophilicity over time (A_{UV} = A_{UV'} < 20°) but has a higher hysteresis and so, more heterogeneities.

4. Discussion

4.1. Comparison of Alcoholic and Aqueous **TiO₂** syntheses

A SiO₂ barrier layer does not induce a better crystallinity of TiO₂ when thick glass supports are used. Indeed with **2 mm** glass, crystallization occurs (TiO₂ 500 Alc/SiO₂ 100 Alc 2 mm) which is not the case when the thickness of the glass is **4 mm** (TiO₂ 500 Alc/SiO₂ 100 Alc). The nature of the glass, perhaps, induces a different alkali gradient/migration. Alkalies seem to be more disturbing in the case of 4 mm glass due to higher concentration in the TiO₂ layer during crystallization.

Due to the absence of crystallinity, the photoactivity of TiO₂ 500 Alc or SiO₂-TiO₂ 500 Alc is very low. In this case, it appears the substrate with a high amount of alkali (sodium and calcium) induces a negative effect [40-42].

Alcoholic synthesis produced less active samples than aqueous synthesis, with or without calcination.

The thickness plays an important role in the catalytic activity [43, 44]. Thicknesses of the active layer between all alcoholic films are similar and the same observation is done for all alcoholic samples (except TiO₂ 500 Alc). The thickness cannot explain the difference of activity between both syntheses because as observed, the mean thickness of alcoholic films (50 nm) is higher than the aqueous films (15 nm) while the activity of these aqueous films is better.

In the latter case, the particles are already in the anatase form in samples prepared through aqueous synthesis (GIXRD) and are thus not disturbed by alkalies during the calcination. As a reminder, this calcination is required for adherence purposes only. The decrease of the activity of aqueous samples with calcination is certainly due to sintering. This phenomenon was already observed for powders from the same synthesis [26] in which sintering as well as rutile formation

occur. In the present study, no rutile is observed, perhaps due to the substrate and alkalis that delay the anatase-rutile transition as they delay the amorphous-anatase transition [40-42]. Moreover, the superhydrophilicity is also better than the superhydrophilicity of alcoholic synthesis. This can be due to the better crystallinity [45]; better crystallinity induces a more efficient electron-hole generation and so a better photoinduced hydrophilicity.

The dopant incorporation does not modify significantly the photoactivity. The amount of Zn, 5 wt%, can perhaps explain the absence of enhancement. Indeed, too much Zn^{2+} with a large band gap induces blocking of the light adsorption of TiO_2 [27-29]. A content of less than 6 wt% [15] can be efficient but in the present cases it does not work. According to literature, the incorporation of Zn^{2+} in sol-gel synthesis already showed to be less efficient than direct ZnO insertion [27].

4.2. Comparison of TiO_2 and ZnO

In methylene blue photodegradation tests, TiO_2 Alc and AQ is less active than ZnO but its superhydrophilicity after the first illumination (AUV) is better. The thicknesses of films cannot explain the difference of activities. Indeed TiO_2 AQ and ZnO thickness are in the same range while the activity are different in some cases and similar in another case.

In addition to this improvement in photocatalytic activity, it was expected that composite films would combine the best photoactivity with the best superhydrophilicity, and better maintain this latter property over time (AUV').

An analysis of the composite films shows that only one sample is composed of ZnO and TiO_2 , namely ZnO 500 Alc/ TiO_2 100 AQ. Indeed, GIXRD shows that only crystallized TiO_2 is deposited on the composite TiO_2 500 AQ/ ZnO 100 or 500 Alc and not crystallised ZnO . More precisely, profilometry revealed that the ZnO (100 or 500 Alc) layer is not (chemically) resistant to the TiO_2 AQ. It can be supposed that the acidity of the TiO_2 dissolves the first ZnO layer

during the deposition of the TiO₂ layer [11]. Moreover, the photoactivity of these composites is equal to the activity of TiO₂ 500 AQ. In contrast, the two layers are well deposited for ZnO 500 Alc/TiO₂ 100 AQ. In that sample, GIXRD confirms the presence of TiO₂ and ZnO and profilometry shows that the TiO₂ layer is well deposited and is not dissolved by ZnO, although the amount of ZnO deposited, the second layer, is low. In this case, the composite is therefore composed of a TiO₂ layer below a very thin layer of ZnO.

Finally, the activity under UV, evaluated by MB degradation, shows that the activity of this composite is very slightly improved compared to TiO₂, due to the very thin layer of ZnO, but it clearly performed below the one of pure ZnO which has the highest activity of any sample.

The superhydrophilicity of the 3 composites is also improved: not after the first illumination (A_{UV} is higher than for TiO₂ 500 AQ) but maintained better hydrophilicity over time (A_{UV} still the same and lower than ZnO 500 Alc and TiO₂ 500 AQ).

4.3. Comparison of the degradation of methylene blue and hydrogen peroxide

The samples tested for H₂O₂ degradation are only the adherent samples and those that have the highest MB degradation. In this case, TiO₂ 500 AQ, ZnO 500 Alc and ZnO 500 Alc/TiO₂ 100 AQ were illuminated with halogen light in H₂O₂ media to produce oxygen. The mechanism of MB blue degradation and hydrogen peroxide degradation are significantly different [7, 38].

The starting point, *i.e.*, the excitation of the photocatalyst, is the same:

- a. Absorption of photons



According to literature, MB is degraded according to the following process [7, 46]:

b. Degradation of methylene blue due to the illumination (=blank test):



c. 1- Oxidation of pollutant R=MB by OH[•]:

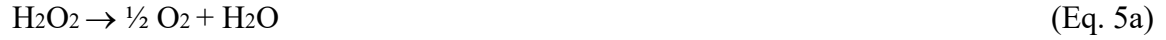


2- Direct oxidation of pollutant by h⁺:



While H₂O₂ is degraded through the following mechanism [38]:

a. Decomposition of H₂O₂ (=blank test)



b. Fenton-like reactions: H₂O₂ gives an electron or accepts an electron from TiO₂, in this case, the semi-conductor catalyses the H₂O₂ decomposition, like iron ions in Fenton reactions [47]



where M can be Ti or Zn.

The different behaviours of photocatalysts seen in response to MB and H₂O₂ tests are difficult to explain because illumination sources and molecules to degrade are different in each case.

Different explanations can be supposed.

The first step of the pollutant degradation is its adsorption on TiO₂ and ZnO which is different depending the pollutant: perhaps MB adsorbs better on ZnO than TiO₂ (for example, due to different sites acidity, site accessibility), while H₂O₂ has perhaps a similar affinity for both catalysts, resulting in the same activity.

Depending upon the illumination, catalysts could be activated differently: in the first test with MB, monochromatic UV-light is used and in the second one with H₂O₂ a continuous UV-Visible spectrum is used. So, following the illumination, e⁻ - h⁺ generation could be not equivalent between the 2 catalysts (only under UV) but could be equivalent under another illumination (under UV-Visible light). This difference in the excitation could come from the difference in the electronic structures and so different band gaps, and also different crystalline structures which can have different e⁻ - h⁺ recombination times.

The better activity of ZnO 500 Alc/TiO₂ 100 AQ under halogen light can perhaps be explained by the interaction of electrons and holes between the band structures of the photocatalysts. Perhaps with this powerful halogen lamp the TiO₂ and ZnO are very well activated. Both pure catalysts have the same activity. In this case it can be supposed that, in the composite, electrons from the conduction band of TiO₂ (or ZnO) can go to the conduction band of ZnO (or TiO₂) and holes can go from the valence band of ZnO (or TiO₂) to the valence band of TiO₂ (or ZnO). There is therefore a decrease in electron-hole recombination inducing a better activity. This enhancement was already observed for composite films of TiO₂ and ZnO during evaluation of the pollutant oxidation potential [13] or the degradation of 4-chlorophenol, where TiO₂ and

ZnO have similar activities while the composite is better [37]. Finally, according to literature [17], TiO₂ is better than the composite and this composite is better than ZnO for degradation of NO_x due to a change in photoconductivity.

5. Conclusion

In this work, pure TiO₂, pure ZnO and TiO₂ doped with Zn have been produced. Films have been produced using an optimized dip-coating process on thick soda-lime glass substrates.

The influence of the dopants on the physico-chemical properties of the catalysts has been investigated using GIXRD, UV-Vis spectroscopy and profilometry. The photocatalytic activity of the different catalysts has been evaluated by monitoring the degradation of methylene blue (MB) under UV light, *p*-nitrophenol under visible light and hydrogen peroxide under halogen light. Superhydrophilicity and aesthetics of films have also been evaluated for each film.

TiO₂ from aqueous synthesis has appeared better than TiO₂ from alcoholic synthesis for superhydrophilicity and photocatalytic activity. The main reason for this was the control of the crystallinity. TiO₂ from alcoholic synthesis, even with a barrier layer, is not crystallized because during calcination, alkali from the substrate have prevented crystallization. Aqueous synthesis did not require this calcination and so alkali did not disturb the crystallization. Aqueous synthesis was therefore more compatible with the use of industrial glass.

Comparison of TiO₂ AQ and ZnO showed that TiO₂ had a better superhydrophilicity after a first UV illumination than ZnO. For photocatalytic activity, different factors influence the activity. First, no activity under visible light for the degradation of *p*-nitrophenol was observed.

Then, depending on the pollutant and the excitation, TiO₂ and ZnO exhibited different activity. The degradation of methylene blue was more efficient with ZnO than with TiO₂ or TiO₂/ZnO, while the degradation of H₂O₂ under halogen light was similar for TiO₂ and ZnO but better for TiO₂/ZnO. From these measurements, the pollutant affinity or the excitation of the catalyst

could be the key factors that influence the yield of the photodegradation. The composite film ZnO 500 Alc/TiO₂ 100 AQ maintained superhydrophilicity over time (AUV') compared to ZnO 500 Alc and TiO₂ 500 AQ, exhibiting slightly higher activity compared to TiO₂ 500 AQ for methylene blue degradation and compared to ZnO 500 Alc and TiO₂ 500 AQ for H₂O₂ degradation. Finally, in all cases, the aesthetic properties of the glass remained the same regardless of the treatment or the coating.

Acknowledgments

The authors thank Lionel Ventelon, from AGC Glass Europe S.A., for the supply of the glass support and the haze measurements. A. Ramírez thanks the FNRS-Belgium (National Council of Scientific Research) and Universidad del Cauca.

References

[1] C.M. Malengreaux, G.M.L. Léonard, S.L. Pirard, I. Cimieri, S.D. Lambert, J.R. Bartlett, B. Heinrichs, How to modify the photocatalytic activity of TiO₂ thin films through their roughness by using additives. A relation between kinetics, morphology and synthesis, *Chemical Engineering Journal* 243 (2014) 537-548.

[2] A. Fujishima, K. Hashimoto, T. Watanabe, *TiO₂ Photocatalysis: Fundamentals and Applications*, BKC, Inc, Tokyo, 1999.

[3] A. Mills, S. LeHunte, An overview of semiconductor photocatalysis, *Journal of Photochemistry and Photobiology a-Chemistry* 108 (1997) 1-35.

[4] A. Ghicov, J.M. Macak, H. Tsuchiya, J. Kunze, V. Haeublein, L. Frey, P. Schmuki, Ion Implantation and Annealing for an Efficient N-Doping of TiO₂ Nanotubes, *Nano Letters* 6 (2006) 1080-1082.

[5] G. Impellizzeri, V. Scuderi, L. Romano, E. Napolitani, R. Sanz, R. Carles, V. Privitera, C ion-implanted TiO₂ thin film for photocatalytic applications, *Journal of Applied Physics* 117 (2015) 105308.

[6] S. Banerjee, D.D. Dionysiou, S.C. Pillai, Self-cleaning applications of TiO₂ by photo-induced hydrophilicity and photocatalysis, *Applied Catalysis B: Environmental* 176-177 (2015) 396-428.

[7] M. Pelaez, N.T. Nolan, S.C. Pillai, M.K. Seery, P. Falaras, A.G. Kontos, P.S.M. Dunlop, J.W.J. Hamilton, J.A. Byrne, K. O'Shea, M.H. Entezari, D.D. Dionysiou, A review on the visible light active titanium dioxide photocatalysts for environmental applications, *Applied Catalysis B: Environmental* 125 (2012) 331-349.

[8] V. Scuderi, G. Impellizzeri, L. Romano, M. Scuderi, G. Nicotra, K. Bergum, A. Irrera, B.G. Svensson, V. Privitera, TiO₂-coated nanostructures for dye photo-degradation in water, *Nanoscale Research Letters* 9 (2014) 458.

[9] I. Udom, M.K. Ram, E.K. Stefanakos, A. Hepp, D. Goswami, One dimensional-ZnO nanostructures: Synthesis, properties and environmental applications, 2013.

[10] Ü. Özgür, Y.I. Alivov, C. Liu, A. Teke, M.A. Reshchikov, S. Doğan, V. Avrutin, S.-J. Cho, H. Morkoç, A comprehensive review of ZnO materials and devices, *Journal of Applied Physics* 98 (2005) 041301.

[11] R. Jose, V. Thavasi, S. Ramakrishna, Metal Oxides for Dye-Sensitized Solar Cells, *Journal of the American Ceramic Society* 92 (2009) 289-301.

[12] A. Solbrand, K. Keis, S. Södergren, H. Lindström, S.-E. Lindquist, A. Hagfeldt, Charge transport properties in the nanostructured ZnO thin film electrode – electrolyte system studied with time resolved photocurrents, *Solar Energy Materials and Solar Cells* 60 (2000) 181-193.

[13] Z. Zhang, Y. Yuan, Y. Fang, L. Liang, H. Ding, L. Jin, Preparation of photocatalytic nano-ZnO/TiO₂ film and application for determination of chemical oxygen demand, *Talanta* 73 (2007) 523-528.

[14] S. Sakthivel, B. Neppolian, M.V. Shankar, B. Arabindoo, M. Palanichamy, V. Murugesan, Solar photocatalytic degradation of azo dye: comparison of photocatalytic efficiency of ZnO and TiO₂, *Solar Energy Materials and Solar Cells* 77 (2003) 65-82.

[15] D. Ramírez-Ortega, A.M. Meléndez, P. Acevedo-Peña, I. González, R. Arroyo, Semiconducting properties of ZnO/TiO₂ composites by electrochemical measurements and their relationship with photocatalytic activity, *Electrochimica Acta* 140 (2014) 541-549.

[16] J. Tian, L. Chen, Y. Yin, X. Wang, J. Dai, Z. Zhu, X. Liu, P. Wu, Photocatalyst of TiO₂/ZnO nano composite film: Preparation, characterization, and photodegradation activity of methyl orange, *Surface and Coatings Technology* 204 (2009) 205-214.

[17] N. Todorova, T. Giannakopoulou, K. Pomoni, J. Yu, T. Vaimakis, C. Trapalis, Photocatalytic NO_x oxidation over modified ZnO/TiO₂ thin films, *Catalysis Today* 252 (2015) 41-46.

[18] T. Giannakopoulou, N. Todorova, M. Giannouri, J. Yu, C. Trapalis, Optical and photocatalytic properties of composite TiO₂/ZnO thin films, *Catalysis Today* 230 (2014) 174-180.

[19] M.S. Lee, S.-S. Hong, M. Mohseni, Synthesis of photocatalytic nanosized TiO₂-Ag particles with sol-gel method using reduction agent, *Journal of Molecular Catalysis A: Chemical* 242 (2005) 135-140.

[20] M. Houmar, D. Riassetto, F. Roussel, A. Bourgeois, G. Berthomé, J.C. Joud, M. Langlet, Morphology and natural wettability properties of sol-gel derived TiO₂-SiO₂ composite thin films, *Applied Surface Science* 254 (2007) 1405-1414.

[21] K. Guan, Relationship between photocatalytic activity, hydrophilicity and self-cleaning effect of TiO₂/SiO₂ films, *Surface and Coatings Technology* 191 (2005) 155-160.

[22] Y. Chen, C. Zhang, W. Huang, C. Yang, T. Huang, Y. Situ, H. Huang, Synthesis of porous ZnO/TiO₂ thin films with superhydrophilicity and photocatalytic activity via a template-free sol-gel method, *Surface and Coatings Technology* 258 (2014) 531-538.

[23] D. Barreca, A. Gasparotto, C. Maccato, E. Tondello, U.L. Štangar, S.R. Patil, Photoinduced superhydrophilicity and photocatalytic properties of ZnO nanoplatelets, *Surface and Coatings Technology* 203 (2009) 2041-2045.

[24] B.-j. Li, L.-j. Huang, M. Zhou, N.-f. Ren, Reversible wettability control of ZnO thin films synthesized by hydrothermal process on different buffer layers, *Materials Letters* 110 (2013) 160-163.

[25] H.Y. He, Photoinduced superhydrophilicity and high photocatalytic activity of ZnO-reduced graphene oxide nanocomposite films for self-cleaning applications, *Materials Science in Semiconductor Processing* 31 (2015) 200-208.

[26] C. Malengreux, S. Douven, D. Poelman, B. Heinrichs, J. Bartlett, An ambient temperature aqueous sol-gel processing of efficient nanocrystalline doped TiO₂-based photocatalysts for the degradation of organic pollutants, *J Sol-Gel Sci Technol* 71 (2014) 557-570.

[27] G. Liu, X. Zhang, Y. Xu, X. Niu, L. Zheng, X. Ding, The preparation of Zn²⁺-doped TiO₂ nanoparticles by sol–gel and solid phase reaction methods respectively and their photocatalytic activities, *Chemosphere* 59 (2005) 1367-1371.

[28] L.G. Devi, B.N. Murthy, S.G. Kumar, Photocatalytic activity of TiO₂ doped with Zn²⁺ and V⁵⁺ transition metal ions: Influence of crystallite size and dopant electronic configuration on photocatalytic activity, *Materials Science and Engineering: B* 166 (2010) 1-6.

[29] X. Lu, J. Jiang, K. Sun, D. Cui, Characterization and photocatalytic activity of Zn²⁺–TiO₂/AC composite photocatalyst, *Applied Surface Science* 258 (2011) 1656-1661.

[30] S. Lambert, C. Cellier, E.M. Gaigneaux, J.-P. Pirard, B. Heinrichs, Ag/SiO₂, Cu/SiO₂ and Pd/SiO₂ cogelled xerogel catalysts for benzene combustion: Relationships between operating synthesis variables and catalytic activity, *Catalysis Communications* 8 (2007) 1244-1248.

[31] B. Braconnier, C.A. Páez, S. Lambert, C. Alié, C. Henrist, D. Poelman, J.-P. Pirard, R. Cloots, B. Heinrichs, Ag- and SiO₂-doped porous TiO₂ with enhanced thermal stability, *Microporous and Mesoporous Materials* 122 (2009) 247-254.

[32] C.M. Malengreaux, S.L. Pirard, J.R. Bartlett, B. Heinrichs, Kinetic study of 4-nitrophenol photocatalytic degradation over a Zn²⁺ doped TiO₂ catalyst prepared through an environmentally friendly aqueous sol–gel process, *Chemical Engineering Journal* 245 (2014) 180-190.

[33] S. Siuleiman, N. Kaneva, A. Bojinova, K. Papazova, A. Apostolov, D. Dimitrov, Photodegradation of Orange II by ZnO and TiO₂ powders and nanowire ZnO and ZnO/TiO₂ thin films, *Colloids and Surfaces A: Physicochemical and Engineering Aspects* 460 (2014) 408-413.

[34] Y. Huang, Y. Wei, J. Wu, C. Guo, M. Wang, S. Yin, T. Sato, Low temperature synthesis and photocatalytic properties of highly oriented ZnO/TiO₂–xNy coupled photocatalysts, *Applied Catalysis B: Environmental* 123–124 (2012) 9-17.

[35] C.C. Pei, W.W.-F. Leung, Photocatalytic degradation of Rhodamine B by TiO₂/ZnO nanofibers under visible-light irradiation, *Separation and Purification Technology* 114 (2013) 108-116.

[36] N. Serpone, P. Maruthamuthu, P. Pichat, E. Pelizzetti, H. Hidaka, Exploiting the interparticle electron transfer process in the photocatalysed oxidation of phenol, 2-chlorophenol and pentachlorophenol: chemical evidence for electron and hole transfer between coupled semiconductors, *Journal of Photochemistry and Photobiology A: Chemistry* 85 (1995) 247-255.

[37] G.S. Pozan, A. Kambur, Significant enhancement of photocatalytic activity over bifunctional ZnO–TiO₂ catalysts for 4-chlorophenol degradation, *Chemosphere* 105 (2014) 152-159.

[38] L. Tasseroul, C.A. Páez, S.D. Lambert, D. Eskenazi, B. Heinrichs, Photocatalytic decomposition of hydrogen peroxide over nanoparticles of TiO₂ and Ni(II)-porphyrin-doped TiO₂: A relationship between activity and porphyrin anchoring mode, *Applied Catalysis B: Environmental* 182 (2016) 405-413.

[39] S.L. Pirard, C.M. Malengreaux, D. Toye, B. Heinrichs, How to correctly determine the kinetics of a photocatalytic degradation reaction?, *Chemical Engineering Journal* 249 (2014) 1-5.

[40] G.L.M. Léonard, C.M. Malengreaux, Q. Mélotte, S.D. Lambert, E. Bruneel, I. Van Driessche, B. Heinrichs, Doped sol–gel films vs. powders TiO₂: On the positive effect induced by the presence of a substrate, *Journal of Environmental Chemical Engineering* 4 (2016) 449-459.

[41] J.M. J. Zita, J. Krysa, Multilayer TiO₂/SiO₂ thin sol-gel films : Effect of calcination temperature and Na⁺ diffusion, *Journal of Photochemistry and Photobiology A:Chemistry* 216 (2010) 194-200.

[42] J. Yu, X. Zhao, Effect of substrates on the photocatalytic activity of nanometer TiO₂ thin films, *Materials Research Bulletin* 35 (2000) 1293-1301.

[43] T. Luttrell, S. Halpegamage, J. Tao, A. Kramer, E. Sutter, M. Batzill, Why is anatase a better photocatalyst than rutile? - Model studies on epitaxial TiO(2) films, *Scientific Reports* 4 (2014) 4043.

[44] A. Di Mauro, M. Cantarella, G. Nicotra, V. Privitera, G. Impellizzeri, Low temperature atomic layer deposition of ZnO: Applications in photocatalysis, *Applied Catalysis B: Environmental* 196 (2016) 68-76.

[45] A.A. Ashkarraan, M.R. Mohammadizadeh, The effect of heat treatment on superhydrophilicity of TiO₂ nano thin films, *Eur. Phys. J. Appl. Phys.* 40 (2007) 155-162.

[46] A. Houas, H. Lachheb, M. Ksibi, E. Elaloui, C. Guillard, J.-M. Herrmann, Photocatalytic degradation pathway of methylene blue in water, *Applied Catalysis B: Environmental* 31 (2001) 145-157.

[47] J. Pignatello, Advanced Oxidation Processes for Organic Contaminant Destruction Based on the Fenton Reaction and Related Chemistry, *Critical Reviews in Environmental Science and Technology* 36 (2006) 1-84.